Plausible phospho*enol*pyruvate binding site revealed by 2.6 Å structure of Mn^{2+}-bound phospho*enol*pyruvate carboxylase from *Escherichia coli*[1]

Hiroyoshi Matsumura[a], Mika Terada[a], Shunsuke Shirakata[a], Tsuyoshi Inoue[a], Takeo Yoshinaga[b], Katsura Izui[c], Yasushi Kai[a,*]

[a] *Department of Materials Chemistry, Graduate School of Engineering, Osaka University, Suita, Osaka 565-0871, Japan*
[b] *Department of Public Health, Graduate School of Medicine, Kyoto University, Sakyo-ku, Kyoto 606-8501, Japan*
[c] *Division of Integrated Life Science, Graduate School of Biostudies, Kyoto University, Sakyo-ku, Kyoto 606-8502, Japan*

Received 31 May 1999; received in revised form 3 August 1999

Abstract We have determined the crystal structure of Mn^{2+}-bound *Escherichia coli* phospho*enol*pyruvate carboxylase (PEPC) using X-ray diffraction at 2.6 Å resolution, and specified the location of enzyme-bound Mn^{2+}, which is essential for catalytic activity. The electron density map reveals that Mn^{2+} is bound to the side chain oxygens of Glu-506 and Asp-543, and located at the top of the α/β barrel in PEPC. The coordination sphere of Mn^{2+} observed in *E. coli* PEPC is similar to that of Mn^{2+} found in the pyruvate kinase structure. The model study of Mn^{2+}-bound PEPC complexed with phospho*enol*pyruvate (PEP) reveals that the side chains of Arg-396, Arg-581 and Arg-713 could interact with PEP.

Key words: Phospho*enol*pyruvate carboxylase; Crystal structure; Mn^{2+}-bound form; Phospho*enol*pyruvate binding site

1. Introduction

Phospho*enol*pyruvate carboxylase (PEPC; EC 4.1.1.31) catalyzes the irreversible carboxylation of phospho*enol*pyruvate (PEP) to form oxaloacetate (OAA) and inorganic phosphate. A divalent metal ion such as Mn^{2+} or Mg^{2+} is essential for enzymatic activity. The enzyme is widespread in higher plants, algae and many kinds of bacteria, and plays an anaplerotic role by replenishing C_4-dicarboxylic acid to the tricarboxylic acid cycle [1–3]. In C_4 plants such as maize and sugarcane and in crassulacean acid metabolism (CAM) plants such as pineapple and cactus, PEPC is a key enzyme in the fixation of atmospheric CO_2.

PEPC from *Escherichia coli* is an allosteric enzyme which is activated by acetyl coenzyme A (CoASc) or fructose 1,6-bisphosphate and inhibited by L-aspartate. Although the first crystal structure of *E. coli* PEPC complexed with L-aspartate was determined in 1999 [4], the reaction mechanism for PEPC has not been determined, because both substrate analogue and divalent metal ion were not complexed with the enzyme within the crystal.

Previous studies suggest that Mn^{2+} or Mg^{2+} can bind to the active site of PEPC even in the absence of PEP [5,6]. Hydrolysis study of PEP by PEPC suggests that the active site metal ion binds to the enolate oxygens of PEP or enolate intermediate [7]. Initially, it is important to determine the metal binding site in the enzyme to clarify the molecular mechanism for catalysis. The following contains the refined crystal structure of Mn^{2+}-bound PEPC from *E. coli*, which reveals the location of Mn^{2+} bound to the active site, and the plausible PEP binding site in the enzyme.

2. Materials and methods

2.1. Purification and crystallization

PEPC from *E. coli* was purified and crystallized as described previously [8], with minor modifications. The mother solution in the 6 μl droplet contained 10 mg/ml protein in 50 mM Tris-HCl (pH 7.4) with 6 mM Na-L-Asp, 45 mM $CaCl_2$, 0.6 mM dithiothreitol (DTT), 0.6 M sucrose, 20 mM $MnSO_4$ and 10% (w/v) polyethylene glycol (PEG) 300. The droplet was equilibrated against a 500 μl reservoir solution containing 2.5 mM Na-L-Asp, 90 mM $CaCl_2$, 0.25 mM DTT, and 15% (w/v) PEG300 in the same buffer. Crystals belonged to the orthorhombic space group of *I*222 with unit cell parameters of $a = 117.7$, $b = 248.4$, and $c = 83.5$ Å, which was isomorphous with the metal-free crystal of PEPC complexed with L-aspartate. The asymmetric unit contained one PEPC monomer.

2.2. Data collection and refinement of structure

X-ray diffraction intensities were measured at station BL18B of the Photon Factory, Tsukuba, Japan, using Sakabe's Weissenberg camera for macromolecular crystallography and imaging plates as a detector [9]. The data were processed using DENZO and scaled with the program SCALEPACK [10]. A total of 157 727 observations were recorded from three crystals and were reduced to 34 597 unique reflections. The data were 90.7% complete to 2.6 Å resolution with an $R_{merge} = 6.6\%$.

The crystal structure of *E. coli* PEPC at 2.8 Å resolution was used as an initial model (Brookhaven Protein Data Bank code, 1FIY) [4]. After rigid body refinement, the initial model was refined with REFMAC [11], and manual modifications of the model structure were performed with the graphics program O [12].

3. Results and discussion

The results of the structural analysis of Mn^{2+}-bound PEPC complexed with L-aspartate are shown in Table 1. During the structure refinement the 5σ ($F_{obs} - F_{calc}$) difference maps phased by the Mn^{2+}-free model at the top of the α/β barrel in PEPC are checked (Fig. 1A). The maps clearly reveal the location of Mn^{2+} bound to carboxylate side chain oxygens of conserved Glu-506 and Asp-543 at the C-terminal end of β-5 and β-6 in eight β-strands of the α/β barrel, respectively. The

*Corresponding author. Fax: +81-6-6879-7409.
E-mail: kai@chem.eng.osaka-u.ac.jp

[1] The coordinates and structure factors have been deposited in the Protein Data Bank (accession number 1QB4).

Abbreviations: PEPC, phospho*enol*pyruvate carboxylase; PEP, phospho*enol*pyruvate; OAA, oxaloacetate; CAM, crassulacean acid metabolism; CoASc, acetyl coenzyme A; PEG, polyethylene glycol; PK, pyruvate kinase; PPDK, pyruvate phosphate dikinase; DCDP, 3,3-dichloro-2-dihydroxyphosphinoylmethyl-2-propenoate

PII: S0014-5793(99)01103-5

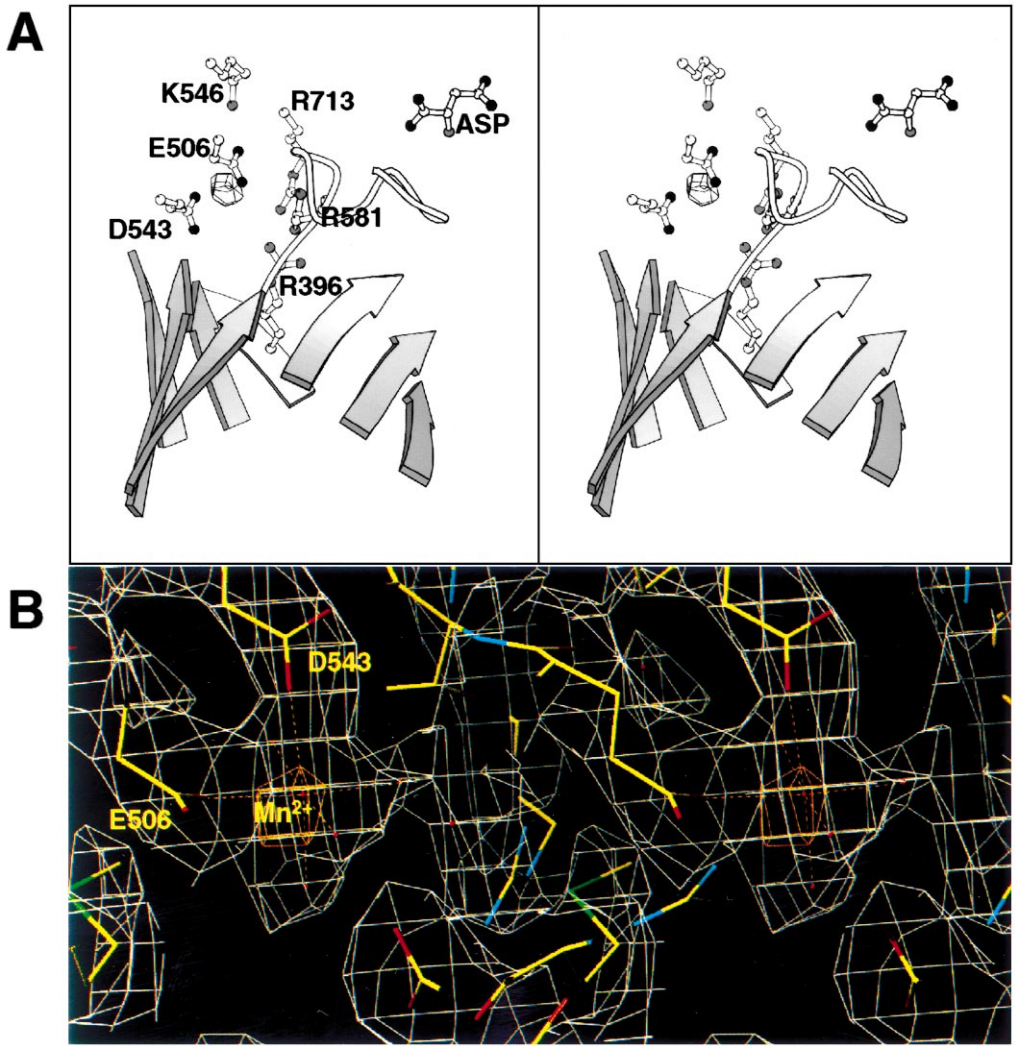

Fig. 1. Stereoview of the active site structure of the monomer PEPC. A: R396, E506, D543, K546, R581, R713 and L-aspartate are shown in ball-and-stick representation. The 5σ ($F_{obs}-F_{calc}$) difference map is phased from the Mn^{2+}-free model in the resolution range of 20–2.6 Å. The figures were produced with MOLSCRIPT [26]. B: The electron density maps around the Mn^{2+} binding site. ($2F_{obs}-F_{calc}$) map contoured at 0.5σ and ($F_{obs}-F_{calc}$) map contoured at 5σ are drawn in white and red, respectively. The four possible water molecules are shown in ball representation. The coordination sphere of Mn^{2+} is approximately octahedral.

coordination sphere of Mn^{2+} is approximately octahedral and four water molecules presumably complete the coordination but are not visible in the electron density at this resolution (Fig. 1B).

Both the PEP binding domains of pyruvate kinase (PK) and pyruvate phosphate dikinase (PPDK) form an α/β barrel [13,14], despite the absence of significant amino acid sequence homology with PEPC. Similarly, PEPC, PK and PPDK, the PEP utilizing enzymes, require divalent cations such as Mn^{2+} or Mg^{2+} for enzymatic activity. A search of protein folds using the complete coordinates of PEPC and protein coordinates in the Protein Data Bank with the program DALI [15] reveals that α/β barrels of PK and PPDK are structurally the most similar to that of PEPC. The Cα atoms in the α/β barrel of PEPC are superimposed on those of PK and PPDK with the rms deviations of 3.60 Å for 212 structurally equivalent α-carbons, and 3.35 Å for 210 structurally equivalent α-carbons. The majority of the overlapping pairs are found in β-5 and β-6 in eight β-strands (Fig. 2A), indicating that the Mn^{2+} binding modes of these enzymes are similar. In fact, the Mn^{2+} binding mode of PEPC is deduced by analogy with that of Mn^{2+}-pyruvate-bound PK. The Mn^{2+}-ligated Glu-271 and Asp-295 in PK are strictly conserved, located at the C-terminal end of β-5 and β-6 in the eight-stranded β-barrel. The same observation is applied to PPDK (Fig. 2B). Although the T-state Mn^{2+}-bound PEPC was presented here, the active site cleft in PEPC would remain unchanged between the T- and R-states, because the comparison between the structures

Table 1
Refinement statistics

Statistic	Value
Resolution (Å)	20–2.6
Number of reflections used	33 439
R_{cryst} (%)	22.1
R_{free} (%)	26.1
Number of non-hydrogen protein atoms	6844
Number of water molecules	81
Rms deviation	
Bond length (Å)	0.017
Bond angle (°)	1.8

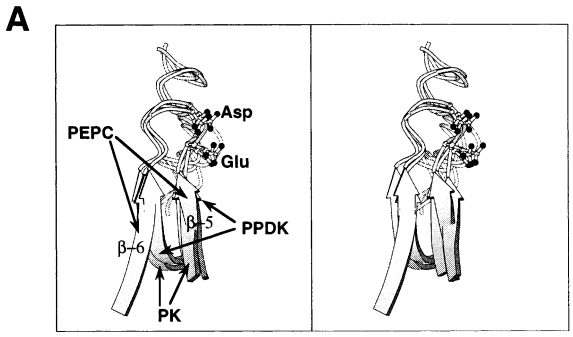

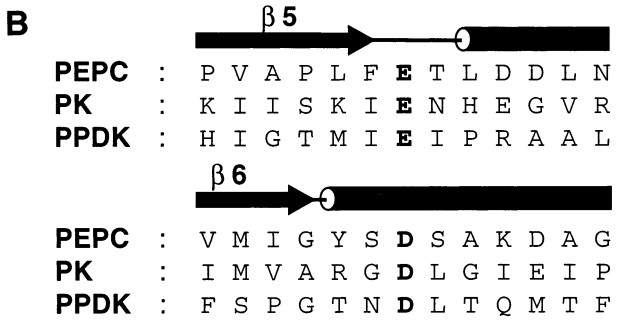

Fig. 2. Comparison of the structure of PEPC with those of PK and PPDK. A: Stereoview of the superposition on β-5, β-6 and the C-terminal region of β-5, β-6. Conserved glutamate and aspartate residues in the enzymes are shown in ball-and-stick representation. B: Amino acid sequence alignment of PEPC, PK and PPDK. The secondary structural elements, determined with the DSSP program [27], are indicated by arrows (β-strands) and cylinders (α-helices). Conserved glutamate (E) and aspartate (D) residues in the three enzymes are shown in bold.
←

of T-state *E. coli* PK [16] and the R-like rabbit muscle enzyme [17] shows that all the amino acids composing the active site cleft display a highly conserved conformation, except for a few conformational changes of side chains. Therefore, the Mn^{2+}-PEP binding modes of these three enzymes seem to be structurally identical.

Similar to rabbit muscle PK [17], PEP can be accommodated close to the center of the α/β-barrel, at the C-terminal end of the β-strands in PEPC (Fig. 3A). The clustering of the negatively and positively charged residues suggests that the phosphoryl and the carboxyl groups of PEP could be kept in this electrostatic environment. Small adjustments in the conformations of two side chains of Asp-543 and Arg-581 are necessary to avoid van der Waals clashes and to facilitate favorable interactions between the side chains of Arg-396, Arg-581, Arg-713 and the phosphoryl group of PEP (Fig.

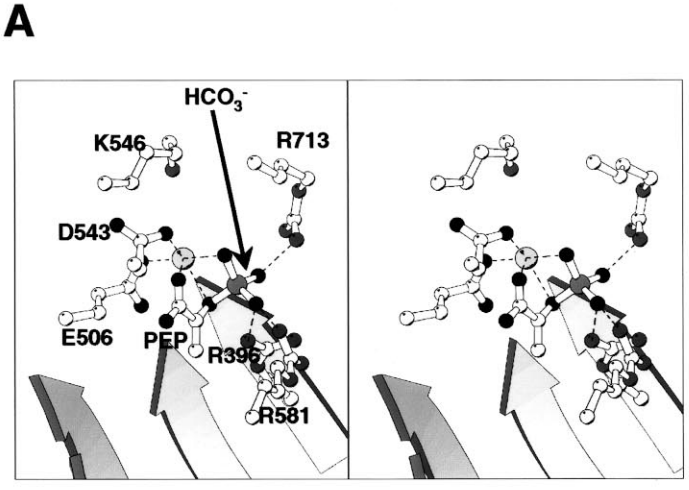

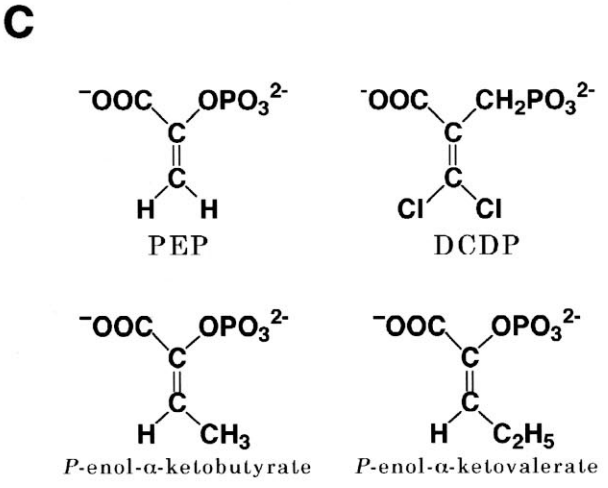

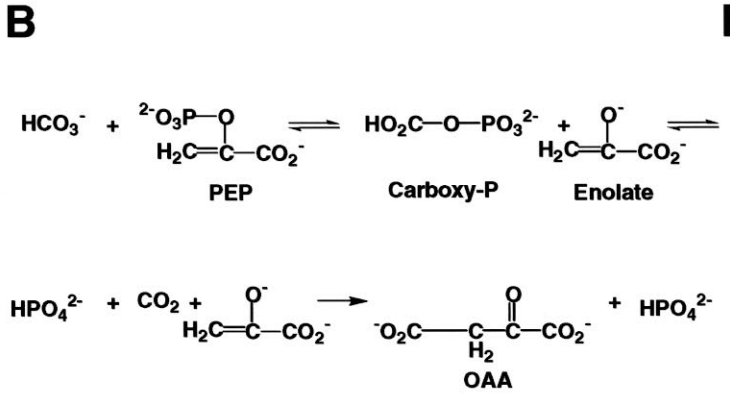

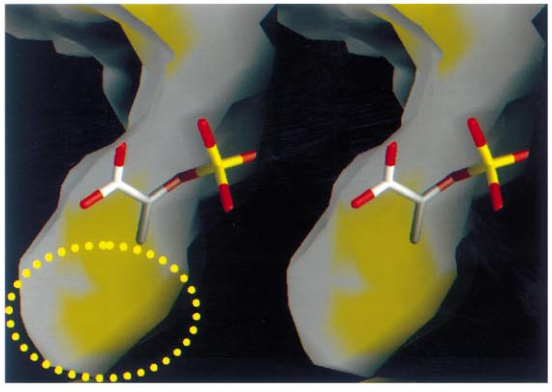

Fig. 3. A: Stereoview of the modeled PEP in the active site of PEPC. The putative HCO_3^- path is shown as an arrow. B: Proposed reaction mechanism of PEPC [3]. C: PEP and its analogues. D: Stereoview of the hydrophobic pocket around the methylene group of PEPC. The hydrophobic pocket consisting of Trp-248, Leu-504 and Met-538 is drawn in yellow. The dashed yellow circle indicates the hydrophobic pocket. The modeled PEP is shown in stick representation. The figures were drawn with GRASP [28].

3A). Arg-396, Arg-581 and Arg-713 are strictly conserved in all PEPCs studied to date [18,19]. Site-directed mutagenesis study on an active site domain performed with *Flaveria trinervia* PEPC suggests that Arg-396 and Arg-713 (*E. coli* numbering) are catalytically essential for PEPC function [20]. Arg-581 is the first arginine residue in a highly conserved sequence, glycine-rich GR^{581}GGXXGRGG, that is unique to PEPC. Fig. 3B shows the proposed reaction mechanism of PEPC [3]. In this mechanism the first chemical step is the nucleophilic attack by bicarbonate to form carboxyphosphate and the enolate of pyruvate. The positively charged electrostatic pocket formed by Arg-396, Arg-581 and Arg-713 would allow for the dissipation of the negative charges of the phosphate group during the approach of the transition state, thereby making the phosphorus atom more electrophilic and susceptible to nucleophilic attack by bicarbonate [21]. Results of site-directed mutagenesis studies on conserved lysine residues suggest that the positively charged side chain of Lys-546 (*E. coli* numbering) might be associated with bicarbonate binding [22,23]. The Nε atom of Lys-546 is positioned about 6 Å from the phosphoryl group in the modeled PEP (Fig. 3A). A substantial cavity connects the Nε atom of Lys-546 and the phosphoryl group in PEP, thus the bicarbonate could be transferred to the phosphoryl group through this pathway (Fig. 3A).

Studies on various PEP analogues suggest the topography of the active site of PEPC. Izui et al. reported that for the *E. coli* enzyme the K_i values of phosphoenol α-ketobutyrate and phosphoenol α-ketovalerate (Fig. 3C) are each approximately about one-tenth the K_m value [24]. Furthermore, 3,3-dichloro-2-dihydroxyphosphinoylmethyl-2-propenoate (DCDP) (Fig. 3C) is reported to show high specificity towards PEPC among PEP-dependent enzymes [25]. This compound is reported to show no inhibition for PK, PPDK, and another PEP-dependent enzymes. The above-mentioned studies suggest the presence of a hydrophobic pocket around the binding site of the methylene group of PEP. As shown in Fig. 3D, the hydrophobic pocket consisting of Trp-248, Leu-504 and Met-538 is found around the methylene group of modeled PEP, although this kind of pocket is not found in either PK or PPDK. Thus, the active site structure is in agreement with the results of the PEP analogue studies.

The results presented here show the probable PEP binding site in PEPC similar to those in the other two PEP utilizing enzymes, that can be explained by the three-dimensional structure of the T-state Mn^{2+}-bound PEPC. Although this finding suggests the first step of the reaction mechanism of PEPC presented in Fig. 3A,B, it is difficult to suggest the second and third steps of the mechanism because the conformational changes of the enzyme would be required to catalyze in those steps. A more detailed mechanism must await the determination of the three-dimensional structure of the R-state enzyme complexed with PEP analogue, which is currently in progress.

Acknowledgements: This study was partially supported by Sakabe Project Tara of the University of Tsukuba and partially by Grant-in-Aid for Science Research on Priority Areas No. 10305065 and for Scientific Research No. 10480157 from the Ministry of Education, Science and Culture, Japan.

References

[1] Utter, M.F. and Kolenbrander, H.M. (1972) in: The Enzymes, 3rd edn. (Boyer, P.D., Ed.), Vol. 6, pp. 117–168, Academic Press, New York.
[2] O'Leary, M.H. (1982) Annu. Rev. Plant Physiol. 33, 297–315.
[3] Chollet, R., Vidal, J. and O'Leary, M.H. (1996) Annu. Rev. Plant Physiol. Plant Mol. Biol. 47, 273–298.
[4] Kai, Y., Matsumura, H., Inoue, T., Terada, K., Nagara, Y., Yoshinaga, T., Kihara, A., Tsumura, K. and Izui, K. (1999) Proc. Natl. Acad. Sci. USA 96, 823–828.
[5] Miller, R.S., Mildvan, A.S., Chang, H.C., Easterday, R.L., Maruyama, H. and Lane, M.D. (1968) J. Biol. Chem. 243, 6030–6040.
[6] Miziorko, H.M., Nowak, T. and Midvan, A.S. (1974) Arch. Biochem. Biophys. 163, 378–389.
[7] Ausenhus, S.L. and O'Leary, M.H. (1992) Biochemistry 31, 6427–6431.
[8] Inoue, M., Hayashi, M., Sugimoto, M., Harada, S., Kai, Y., Kasai, N., Terada, K. and Izui, K. (1989) J. Mol. Biol. 208, 509–510.
[9] Sakabe, N. (1991) Rev. Sci. Instrum. 66, 1276–1281.
[10] Otwinowski, Z. (1993) Proceedings of CCP4 Study Weekend: DATA Collection and Processing (Sawyer, L., Isaacs, N. and Bailey, S., Eds.), pp. 56–62, Daresbury Laboratory, Warrington.
[11] Murshudov, G.N., Vagin, A.A. and Dodson, E.J. (1997) Acta Crystallogr. D 53, 240–255.
[12] Jones, T.A., Zou, J.Y., Cowan, S.W. and Kjeldgaard, M. (1991) Acta Crystallogr. A 47, 110–119.
[13] Larsen, T.M., Laughlin, L.T., Holden, H.M. and Rayment, I. (1994) Biochemistry 33, 6301–6309.
[14] Herzberg, O., Chen, C.C.H., Kapadia, G., Mcguire, M., Carroll, L.J., Noh, S.J. and Dunaway-Mariano, D. (1996) Proc. Natl. Acad. Sci. USA 93, 2652–2657.
[15] Holm, L. and Sander, C. (1993) J. Mol. Biol. 233, 123–138.
[16] Mattevi, A., Valentine, G., Rizzi, M., Speranza, M.L., Bolognesi, M. and Coda, A. (1995) Structure 3, 729–741.
[17] Larsen, T.M., Benning, M.M., Wesenberg, G.E., Rayment, I. and Reed, G.H. (1997) Arch. Biochem. Biophys. 345, 199–206.
[18] Toh, H., Kawamura, T. and Izui, K. (1994) Plant Cell Environ. 17, 31–43.
[19] Nakamura, T., Yoshioka, I., Takahashi, M., Toh, H. and Izui, K. (1995) J. Biochem. (Tokyo) 118, 319–324.
[20] Gao, Y. and Woo, K.C. (1996) FEBS Lett. 392, 285–288.
[21] Westheimer, F.H. (1987) Science 235, 1173–1178.
[22] Dong, L.Y., Ueno, Y., Hata, S. and Izui, K. (1997) Plant Cell Physiol. 38, 1340–1345.
[23] Gao, Y. and Woo, K.C. (1995) FEBS Lett. 375, 95–98.
[24] Izui, K., Matsuda, Y., Kameshita, I., Katsuki, H. and Woods, A.E. (1983) J. Biochem. (Tokyo) 94, 1789–1795.
[25] Jenkins, C.L.D., Harris, R.L.N. and McFadden, H.G. (1986) Biochem. Int. 14, 219–226.
[26] Kraulis, P. (1991) J. Appl. Crystallogr. 24, 946–950.
[27] Kabsch, W. and Sander, C. (1983) Biopolymers 22, 2577–2637.
[28] Nicholls, A., Sharp, K.A. and Honig, B. (1991) Proteins 11, 281–296.